293 A Background

In this section, we describe Generative Flow Networks in detail (Section A.2), and we perform a survey of related work that tackles the catalyst discovery problem (Section A.3).

A.1 Catalysts for hydrogen energy storage

Hydrogen Energy Storage (HES) is a scalable, sustainable option for storing excess energy for later use. Although HES has a relatively low efficiency compared to alternatives such as pumped storage hydroelectricity and battery storage [42, 31, 6], it is more scalable and transportable than the alternatives. HES via water electrolysis (water-splitting) can be thought of as two half-cell reactions: the hydrogen evolution reaction and the oxygen evolution reaction. Both HER and OER are electrochemical reactions which occur in the catalyzer at different electrodes. While HER is a one-step reaction, OER consists of four intermediate reactions which, under an applied voltage, produces oxygen gas, protons and electrons under acidic conditions. HER, in this setting, brings electrons and protons together to produce hydrogen gas. As the energy is used for water electrolysis, the hydrogen gas can be collected and stored in tanks, or other storage containers. When the energy is in demand again, fuel cells can extract the energy from the stored hydrogen at about 60% efficiency [14]. An efficient catalyst, used in the fuel cell or in the electrocatalyzer, can significantly speed up the reaction rate and improve the efficiency of the process [42].

310 A.2 Generative Flow Networks

A generative flow network (GFlowNets, GFN) is an inference method introduced by [4] that allows one to sequentially construct objects with probability proportional to a non-negative reward function. They have been employed in tasks such as molecule generation, crystal generation, and for causal discovery [22, 1, 3]. A desirable capability of GFlowNets is their ability to generate a diversity of objects that all have high reward (relative to other possible candidates in the space). Within catalyst discovery, this is key, as the reward function may not capture all the relevant predictors of whether a material will be a good catalyst. For example, the reward function may capture a target adsorption energy for the catalyst, but not its stability, which is an important trait (high stability) if the catalyst is to be used in real-world applications. After generating a variety of high-reward catalyst materials, one or more of these materials may also be found to be stable during experimental testing. Furthermore, GFlowNets perform particularly well in cases where the search space is quite large, and outperform methods such as MCMC and reinforcement learning in terms of mode mixing [5].

A key component of GFlownets is the proxy model, which is how the GFlowNet obtains information on the reward landscape, and hence what "desirable", high-reward samples are. Proxy models in our context are predictive models (possibly machine learning models) that allow one to evaluate the reward of a particular sampled object. In the case of molecule or crystal discovery, it may be that the sampled molecule or crystal does not exist in any database, and as such, relevant properties of the crystal must be computed in real time instead. Here, we note that for certain properties such as the formation energy of a crystal, physics simulations such as density functional theory (DFT) are traditionally performed. These simulations are computationally expensive and not scalable to high batch sizes. Hence, a machine learning model that is able to replace the physics simulation and compute the properties of interest is valuable; for crystals, there are many works that develop machine learning-based approaches to compute properties such as formation energy and adsorption energy [35, 36, 13, 9].

Crystal GFlowNet is a GFlowNet designed to discover new materials by sequentially sampling crystal structures [1]. This work uses the GFlowNet paradigm to construct and sample crystal structures that have a high reward. The authors test the method on a reward based upon formation energy, where a high reward corresponds to a low formation energy, and a low reward corresponds to a high formation energy. This allows the framework to be used to sample thermodynamically stable materials with desirable properties. As mentioned earlier, the reward function may use any measurable (or predicted, via a proxy model) characteristic of the material. Sequential crystal construction proceeds in three steps. First, the space group (symmetry operations) of the crystal are selected. Then, the composition (elements and their ratios), and finally, the lattice parameters, which determine the shape of the final lattice. Atom positions are not sampled by the model.

A.3 Machine learning for catalyst discovery 345

352

353

354

355

356

357

358

359

360

361

362

Since traditional catalyst design methods are time-consuming and involve trial and error experiments 346 within a very large search space [18], scientists are turning to machine learning approaches to more efficiently explore the space of good catalysts. Recent work has leveraged both predictive 348 models (which evaluate the performance of catalysts based on their measurable attributes) and 349 generative models (which aim to construct catalyst representations with desirable properties) for 350 catalyst discovery. 351

One major thread of predictive machine learning for catalyst design are predictive models to replace density functional theory (DFT) calculations of adsorption energies. The Open Catalyst Dataset 2020 [8] and 2022 [37] are datasets of 1.2 million and 62 thousand relaxations respectively. The datasets span a wide variety of materials, surfaces and adsorbates, with the inclusion of oxides in OC22. Machine learning models such as FAENet, Schnet, PaiNN, and Graphormer [13] are neural networks (e.g. graph neural networks, transformers) that can be trained to perform the OC20 Initial Structure to Relaxed Energy (IS2RE) task, which involves predicting the relaxed energy of an adsorbate-catalyst system from their initial atomic positions. Machine learning models have also been used to predict formation energies, perform relaxations, predict forces [9]. Predictive machine learning models have also been used to predict the thermodynamic stability of catalysts [44]. All of these predictive models have the potential to be included as proxy models within generative approaches. 363

Recent generative approaches to catalyst discovery include reinforcement learning [23], large lan-364 guage models [24], variational autoencoders [34], and generative adversarial networks (GANs, 365 citation) which aim to generate catalysts de novo, by meeting criteria such as target adsorption 366 energies and encoding this in the reward or loss. AdsorbRL [23] employs Deep Q-learning to find 367 compositions of catalysts that have either minimal or maximal adsorption energy. They only model 368 composition, omitting space groups, crystal symmetries, surface selection, and atom positions. [34] 369 370 addresses the problem by employing a VAE to generate catalysts by sampling from the latent space, but we note that reliance on the latent space makes controllable generation and systematic exploration 371 of possible catalysts difficult. [20] takes the approach of GANs to generate catalysts for the ammonia 372 formation reaction, but does not take catalyst stability into account during generation. LLM-based 373 tools such as [24, 30] have so far been mainly applied to help screen known catalysts and perform a 374 375 literature search.

B Effect of relaxation on lattice parameters

382

383

384

After the GFlowNet generates samples, we relax them using M3GNet PES [9], as detailed in Section 2.1. Figure 3 demonstrates the change in lattice parameters of the cubic platinum lattice before and after relaxation. We note that the lattice parameters relax to the minimum of the total energy of the system.

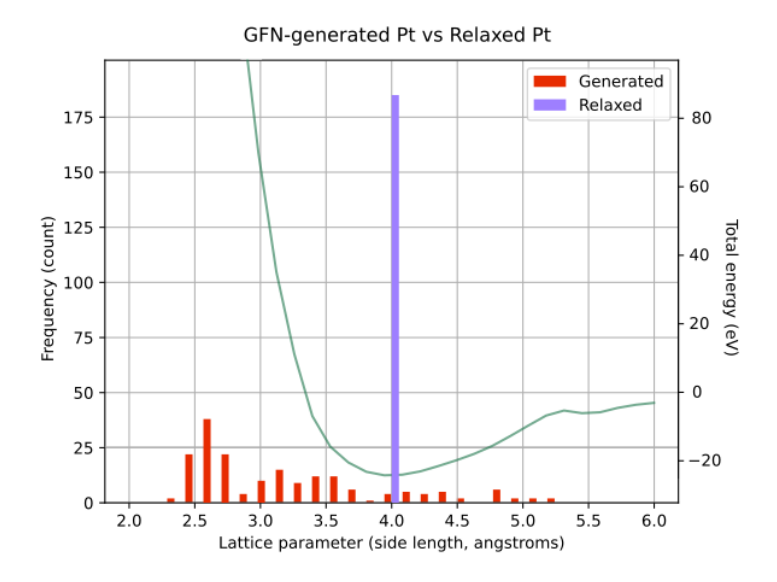


Figure 3: For the HER case study, the platinum samples generated by the GFlownet relax to the minimum energy every time. The green line represents the total energy of the system.

Table 1 details the search space for the Hydrogen evolution reaction case study (Section 2.2). We note that in general, the Catalyst GFlowNet's constraints and search space can be set to be much larger than that used in the HER case study. In future work, we will consider a larger search space up to 80-100 atoms, more elements and space group options, while enforcing a neutral charge constraint.

Table 1: Hydrogen evolution reaction catalyst search space.

Setting	Value	Units
Possible elements	Pt, Ag, Au, Pd, Ir, Ni, W, Co, Cu, Mo, Rh, Nb	
Min. # of different elements in unit cell	1	
Max. # of different elements in unit cell	1	
Min. atoms in unit cell	2	
Max. atoms in unit cell	4	
Min. atoms per element	2	
Max. atoms per element	4	
Enforce neural charge?	No	
Possible space groups	225, 229	
Min. lattice parameter length	2	Angstroms
Max. lattice parameter length	6	Angstroms
Min. angle between lattice vectors	60	Degrees
Max. angle between lattice vectors	140	Degrees

Table of hydrogen evolution reaction samples

Table 2: Proportions of sampled structures for the case study: hydrogen evolution reaction.

		Overpotential (eV)		Samples		
Composition	Space Group	Experimental ²	DFT	Proxy Model	Count	Percentage
Pt	225	0.016	0.03	0.04	185	43.53
Rh	225	0.071^*	0.06	0.03	144	33.88
Pd	229	0.036^{*}	0.09^{*}	0.12	54	12.71
Co	225	0.224^{*}	0.25	0.16	24	5.65
Ir	225	0.015	0.08	0.14	10	2.35
Mo	229	0.394^{*}	0.53	0.21	5	1.18
Cu	225	0.445	0.27	0.39	3	0.71
W	229	0.318*	0.59	0.30	0	0.00
Nb	229	0.488^*	0.56	0.35	0	0.00
Ni	229	0.268	0.23	0.32	0	0.00
Au	225	0.337	0.63	0.51	0	0.00
Ag	225	0.403	0.58	0.62	0	0.00
Sum					425	100.00

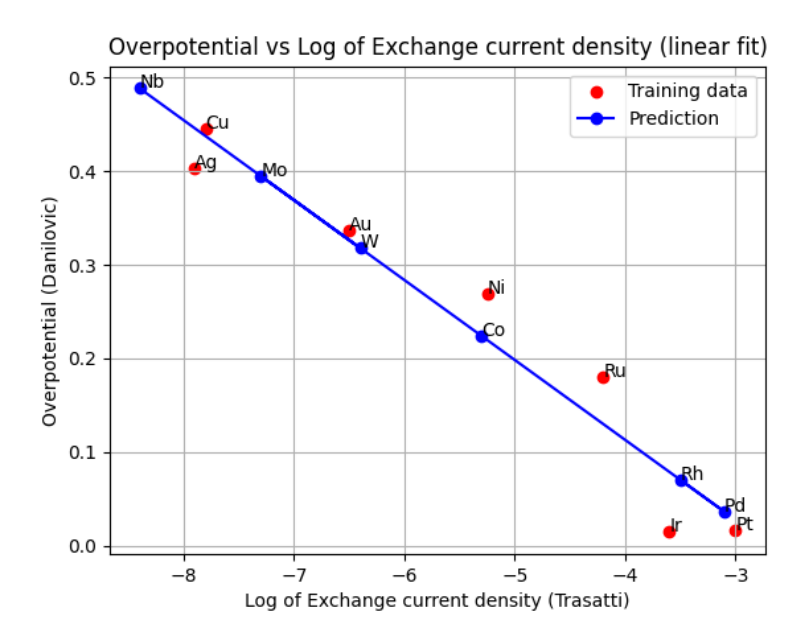


Figure 4: A linear fit that maps log of exchange current density to experimental overpotential using data from [38] and [11]. These values are used column 3 (from the left) of Table 2.

²When available, the experimental overpotential was added from [11]. For the remaining elements, marked with an asterisk, the overpotentials were inferred using a linear fit between the log of experimental exchange current density (from [38]) and the available experimental overpotentials (from [11]). Figure 4 shows the linear fit and predictions.